LABORATORI NAZIONALI DI FRASCATI
SIS – Pubblicazioni

**LNF–95/028 (P)**
**30 Maggio 1995**

# DAΦNE and the Experimental Program

**S. Bianco**
**INFN – Laboratori Nazionali di Frascati, P.O.Box 13, I–00044 Frascati, Italy**

**Abstract**

**The DAΦNE ϕ–factory and the FINUDA and KLOE experiments are reviewed, and their status reported.**

**PACS.: 13.20.Eb; 13.65.+i; 29.20.Dh; 21.80.+a**

Invited Talk given at the
*23rd INS Symposium on Nuclear and Particle Physics with K Beams in the 1 GeV/c Region*
March 15-18, Tokyo, 1995

# 1 Introduction

The $e^+e^-$ collider facility, proposed in 1990 [1] and rapidly approved, it is now being built at the Laboratori Nazionali di Frascati of INFN. The $DA\Phi NE$ collider will operate at the center of mass energy of the $\phi$ meson with an initial luminosity $\mathcal{L} = 1.3 \times 10^{32} cm^{-2} s^{-1}$ and a target luminosity $\mathcal{L} = 5.2 \times 10^{32} cm^{-2} s^{-1}$.

The $\phi(1020)$[2] meson [$s\bar{s}$ quark assignment, mass $m = 1019.413 \pm 0.008\, MeV$, total width $\Gamma = 4.43 \pm 0.06\, MeV$, electronic width $\Gamma_{ee} = 1.37 \pm 0.05\, keV$, and $I^G(J^{PC}) = 0^-(1^{--})$ quantum numbers] is produced in $e^+e^-$ collisions with a

$$\sigma(e^+e^- \to \phi) \sim 5\mu b$$

peak cross section, which translates into a production rate of

$$R_\phi = (5 \times 10^2 \to 2.0 \times 10^3) s^{-1}$$

from initial to target luminosity. The production cross section $\sigma(e^+e^- \to \phi)$ should be compared with the hadronic production, which, in this energy range and for $\beta \to 1$, is given by

$$\sigma(e^+e^- \to f\bar{f}) = \frac{4\pi\alpha^2}{3s} Q_f^2 = \frac{86.8 Q_f^2\, nb}{s[GeV^2]} = 83nb,$$

where $Q_f$ is the charge of the fermion in units of the proton charge, i.e., with an integral S/N ratio of about 30:1.

The $\phi$ then decays at rest into $K^+K^-$ (49%), $K_S^0K_L^0$ (34%), $\rho\pi$ (13%), $\pi^+\pi^-\pi^0$ (2.5%) and $\eta\gamma$ (1.3%). Therefore, a $\phi$-factory is a unique source of monochromatic (110 and 127 MeV/c, respectively), collinear, quantum-defined and tagged neutral and charged kaons. Detecting one K out of the two produced in the $\phi$ decay determines the existence and direction of the other ("tagging").

Two experiments have been approved and are being built: FINUDA, for studying nuclear interactions of the kaons from the $\phi$ decay in a thin target; and KLOE, with the main aim of detecting CP violation in the $K_SK_L$ system. These two lines of study have nothing in common but the exploitation of neutral and charged kaons produced in a unique environment. The description of $DA\Phi NE$ and its physics is very well-suited to the context of this Symposium.

# 2 $DA\Phi NE$

The $DA\Phi NE$ $\phi$-factory machine [6][7][8] in construction at Frascati will make electrons and positrons to collide at the center-of-mass energy of the $\phi$ meson, with a phase I luminosity (begin 1997) of $\mathcal{L} = 1.3 \times 10^{32} cm^{-2} s^{-1}$ with at least 30 bunches, and a final design luminosity of $\mathcal{L} = 5.2 \times 10^{32} cm^{-2} s^{-1}$. To reach phase I luminosity itself is by no means a trivial task, since $1 \times 10^{31} cm^{-2} s^{-1}$ is the max routine luminosity ever attained at $\phi$ meson mass energy (VEPP-2M [9][10]), a one-order of magnitude improvement is necessary.

Table 1: $DA\Phi NE$ single-bunch collision parameters.

| | | | |
|---|---|---|---|
| n bunches | 120 | $\xi$ beam-beam tune shift | 0.04 |
| $\kappa \equiv \sigma_y/\sigma_x$ emitt. ratio | 0.1 | $< i_b >_{max}$ $[mA]$ | 43.7 |
| $\sigma_z$ $[m]$ | 0.03 | $E$ $[MeV]$ | 510 |
| $f_0$ $[MHz]$ | 3.07 | $\epsilon_{max}$ $[m][rad]$ | $10^{-6}$ |
| $\beta_y$ $[m]$ | 0.045 | $N_{max}/bunch$ | $8.9 \times 10^{10}$ |
| $\theta_x$ $[mrad]$ | $10 \div 15$ | $U_0$ $[keV]$ En. loss/turn | 9.3 |

Under a number of simplifying assumptions [11], the luminosity $\mathcal{L}$ of a machine with two separate rings can be expressed as

$$\mathcal{L} = n\mathcal{L}_0,$$

where $n$ is the number of bunches, and $\mathcal{L}_0$ is the single bunch luminosity given by the formula

$$\mathcal{L}_0 = \pi \left(\frac{\gamma}{r_e}\right)^2 f_0 \frac{\xi^2 \epsilon (1+\kappa)}{\beta_y} \tag{1}$$

where $r_e$ is the classical electron radius, $\gamma$ the beam particle energy in units of its rest mass, $\xi$ the beam-beam tune shift parameter, $\kappa$ the coupling factor, $f_0$ the revolution frequency, and $\epsilon$ the emittance. High luminosity $\mathcal{L}$ can be attained either by aiming at high $\mathcal{L}_0$ or by increasing the number of bunches $n$ and keeping $\mathcal{L}_0$ relatively low. The strategy followed is to increase the number of bunches up to $n = 120$, while keeping the single-bunch parameters in eq. 1 quite conservative (table 1). The beam-beam tune shift parameter is, indeed, kept at a comfortable 0.04, which represents what has been achieved with the past and present colliders.

Increasing the number of bunches produces parasitic crossings outside the two interaction regions, which are circumvented by using two separate rings. In $DA\Phi NE$ the electron and positron rings are coplanar, and tangent in the two interaction regions.

The $DA\Phi NE$ complex is sketched in fig.1. $DA\Phi NE$ will be housed in the existing (formerly ADONE) buildings. Electrons and positrons are first accelerated by a linac, stored in an accumulator/damping ring, and finally injected through transfer lines into the main rings. A beam test area and a synchrotron radiation facility complete the accelerator complex.

The linac can deliver electron and positron beams at 50Hz. Manufactured by TITAN-BETA[12], it accelerates electrons to 800 MeV and positrons to 550 MeV. The linac was factory tested in August 1994, delivery was completed in January 1995, and it is now being assembled in Frascati. Full operation is expected to start in December. The beginning of linac operation is particularly interesting, since it will provide - by June 1996 - beams for the calibration of detector subcomponents in a dedicated test area.

The 32.56-m-long accumulator/damping ring stores at 50 Hz the particles in one RF bucket and also damps the transverse and longitudinal emittance of the linac beams. Ring assembly will start in September 1995, and commissioning is expected to begin in February 1996.

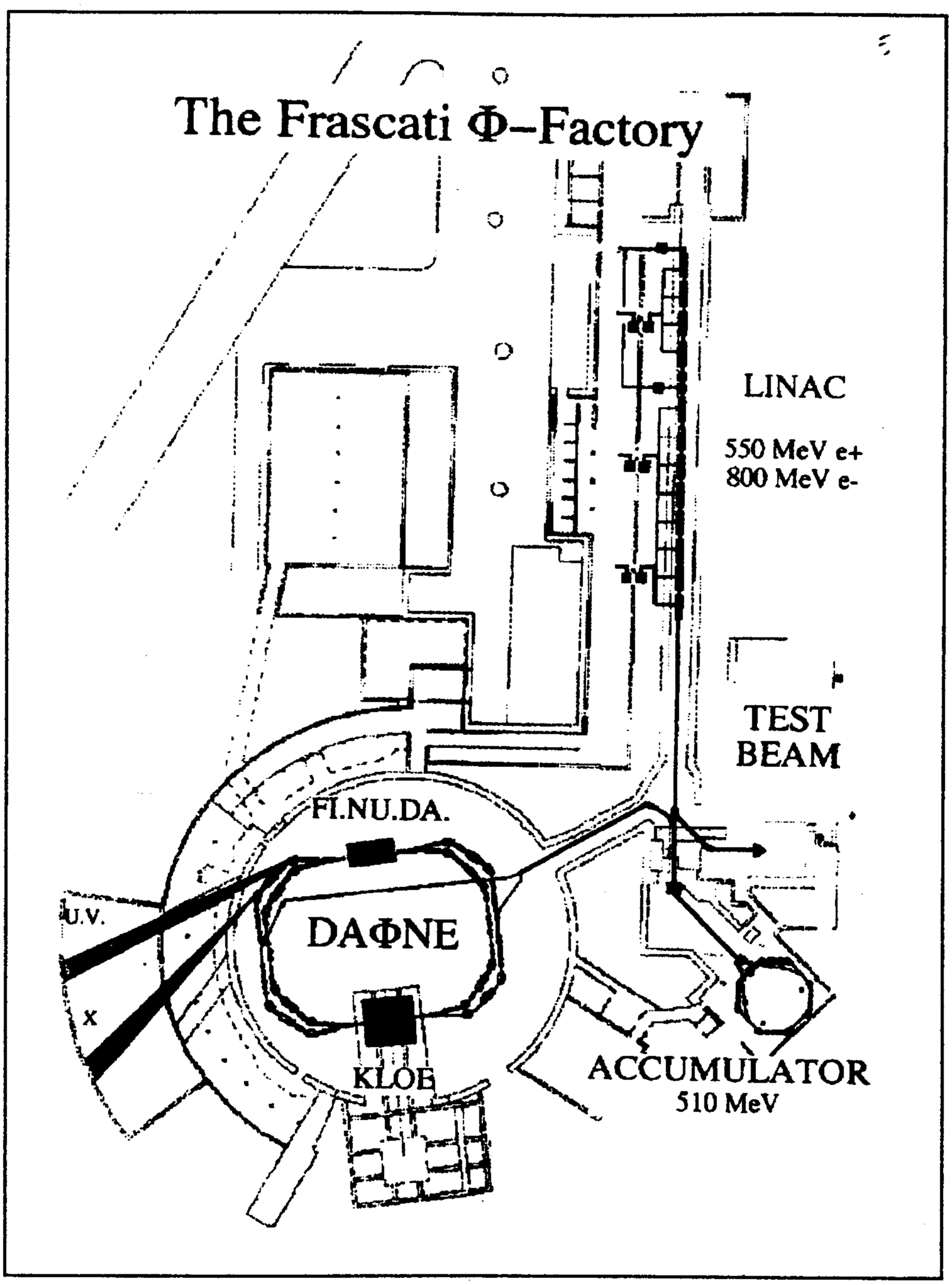


Figure 1: Layout of the $DA\Phi NE$ accelerator complex

Table 2: Beam particles lost by Touschek scattering.

| Scraper aperture $[\sigma_x]$ | Scraper aperture [mm] | Particles lost [part/(s bunch beam)] | Beam lifetime [min] |
|---|---|---|---|
| KLOE at IP=± 43 mm | | | |
| 9 | 25.0 | 0 | 161 |
| 10 | 27.8 | $7.5 \times 10^3$ | 184 |
| $\infty$ | 43.0 | $2.2 \times 10^5$ | 184 |
| FINUDA at IP=± 53 mm | | | |
| 8 | 23.5 | 225 | 141 |
| 9 | 26.5 | $1.7 \times 10^3$ | 161 |
| 10 | 29.4 | $8.7 \times 10^3$ | 184 |
| $\infty$ | 43.0 | $1.0 \times 10^5$ | 184 |

Once inside $DA\Phi NE$ 's main rings, electrons and positrons travel in two separated, coplanar storage rings, colliding at a half-angle of $\theta_x = 10-15\,mrad$ in two interaction points. The design is based on conventional technology, *albeit* pushed to technological challenges by the high-current requirement: the components allow operation at a maximum 5 A current. Each ring contains four normal-conducting wiggler magnets that increase the radiated energy and help tune the beam emittance. Delivery of all main ring magnets is expected within April 1996. Main-ring commissioning is expected to start in December 1996.

The two interaction regions will house the FINUDA and KLOE experiments. Both detector solenoids, with their $\sim 2.4\,T\,m$ integrated field, are a source of large perturbation to the beams. Therefore, three equivalent designs [13] for compensators have been developed to compensate for FINUDA, KLOE, and the so called 'day-one' configuration when the detectors have not yet been installed. Two pairs of permanent compact-size low-$\beta$ quadrupoles and two pairs of conventional solenoids are used for FINUDA, while only permanent quadrupoles are used for the KLOE interaction region. The KLOE experiment requires (see §4) a spherical, large-aperture, Be vacuum chamber.

Particularly interesting from the experimental point of view are the control and limitation of machine background, as simulated in [14], and its connection with the machine lifetime. A scraper system allows one to reduce the rate of particles lost in the detector quadrupoles because of the Touschek effect and thus background such as beam particles showering in the quadrupoles. The number of beam particles lost per second per bunch per beam is shown in table 2 as a function of the scraper aperture in units of horizontal beam rms width, along with the beam lifetime. The rate is by no means negligible, since a fraction of the lost particles will interact inside the detectors and possibly overlap with triggered events. This was carefully studied by both FINUDA and KLOE, to make sure it only marginally affects event pattern recognition.

# 3 FINUDA

Nuclear physics topics will be investigated by the FINUDA (standing for *FIsica NUcleare a DAΦne*) experiment[1]. A nuclear physics experiment carried out at an $e^+e^-$ collider sounds contradictory in itself, but this is where the uniqueness of the idea lies [15]: charged kaons from $\phi$ decays are used as a monochromatic, slow (127 MeV/c), tagged, background-free, high-counting rate beam on a thin target surrounding the beam pipe. The possibility of stopping low-momentum monochromatic $K^-$ with a thin target (typically $0.5\,g\,cm^{-2}$ of $^{12}C$) is unique to $DA\Phi NE$ : $K^-$'s can be stopped with minimal straggling very near the target surface, so that outgoing prompt pions do not cross any significant amount of the target and do not undergo any momentum degradation. This feature provides unprecedented momentum resolution as long as very transparent detectors are employed before and after the target.

The FINUDA detector is optimized to perform high-resolution studies of hypernucleus production and non-mesonic decays[16], by means of a spectrometer with the large acceptance typical of collider experiments. Furthermore, contrary to fixed-target experiments, the direction of the $K^-$ is competely tagged by the detection of the $K^+$ and viceversa.

Negative kaons stopping inside the target produce a $Y$-hypernucleus ($Y = \Lambda, \Sigma, ...$) via the process

$$K^-_{stop} + {}^{A}Z \rightarrow {}^{A}_{Y}Z + \pi^-,$$

where the momentum of the outgoing $\pi^-$ is directly related to the level of the hypernucleus formed (two-body reaction). In the case of $\Lambda$ hypernucleus formation, the following weak-interaction 'decays' are strongly favored in medium-heavy nuclei

$$\Lambda + n \rightarrow n + n \qquad\qquad \Lambda + p \rightarrow n + p,$$

with the nucleus undergoing the reactions

$${}^{A}_{\Lambda}Z \rightarrow {}^{(A-2)}Z + n + n \qquad\qquad {}^{A}_{\Lambda}Z \rightarrow {}^{(A-2)}(Z-1) + n + p,$$

which are interesting for studying the validity of the $\Delta I = 1/2$ rule.

Besides studies on hypernucleus spectroscopy, interest exists for K-N interactions at low energy [17], and for the measurement of the KN scattering length for kaonic-hydrogen X-rays [18]. There exist interesting similarities in the expected rates between FINUDA and the proposed facility at the BNL AGS, where the $(K^-, \pi^\circ)$ reaction, complementary to FINUDA's $(K^-, \pi^-)$ is studied with $K^-$ at rest; both experiments have a design energy resolution below 1 MeV fwhm and a comparable hypernuclei production rate. However, AGS operates with extracted beams at a high rate ($2 \times 10^4 s^{-1}$ stopped $K^-$) and low geometrical acceptance (about 20 msr), while FINUDA's flux, at initial $DA\Phi NE$ luminosity, is two orders of magnitude lower, and the acceptance is 2 orders of magnitude larger. The AGS choice of considering neutral prompt pions is dictated by their use of thick targets, which makes the resolution for emerging prompt charged pions much worse than for neutral pions.

---

[1] FINUDA is on Internet `http://www.lnf.infn.it/esperimenti/finuda/finuda.html`

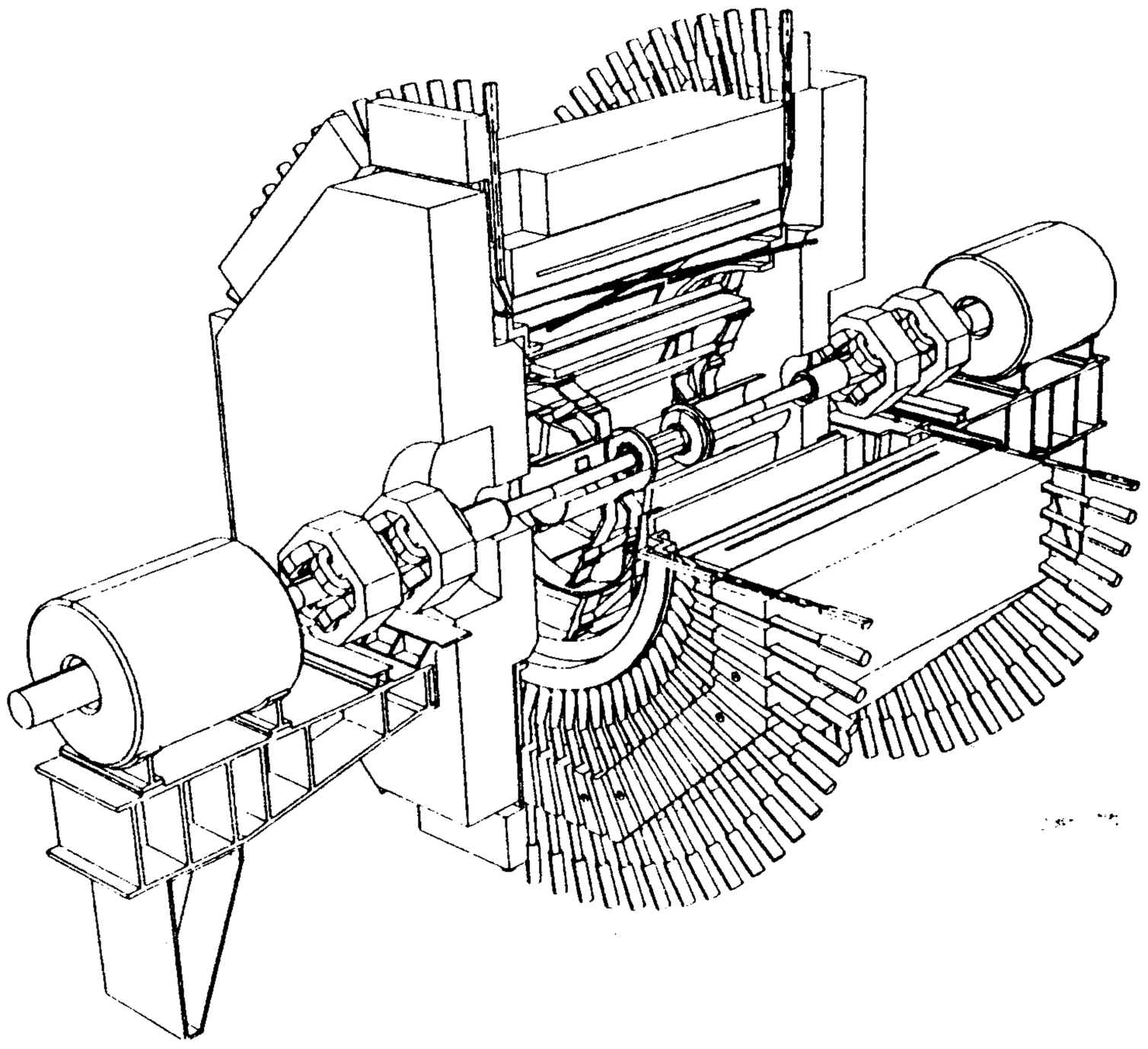

Figure 2: Cut-out view of the FINUDA spectrometer, showing also a section of the $DA\Phi NE$ beam pipe and compensating quadrupoles.

Following the initial idea [15], FINUDA was formally proposed in May 1993 [19], rapidly approved, and funded at the end of 1993. A technical report[20] is to appear shortly as a LNF preprint. For a recent review see [21].

## 3.1 The Apparatus

FINUDA (fig.2) is a magnetic spectrometer with cylindrical geometry, optimized in order to have large solid-angle, optimal momentum resolution (of the order of 0.3 % fwhm on prompt pions) and good triggering capabilities. The geometrical acceptance is approximately $135^0 \leq \vartheta \leq 45^0$, thus naturally rejecting $e^+e^-$ background from Bhabha scattering.

FINUDA consists of (fig.3) an interaction/target region, external tracker, outer scintillator array, and superconducting solenoid. The $(K^+, K^-)$ pairs from $\phi$ decay emerge from the interaction region, whose dimensions are $\sigma_x = 2$ mm, $\sigma_y = 0.02$ mm, $\sigma_z = 3$ cm. The $(K^+, K^-)$ pairs follow a $sin^2\vartheta$ law, with $\vartheta$ the angle relative to the $z$-axis.

The FINUDA magnet is a superconducting solenoid whose magnetic axis is along the beam direction; it provides a highly uniform $B_{max} = 1.1$ T magnetic field (max disuniformity of 5% at the outer edges of the tracking volume). The tracking volume is generated by rotating a trapezium with bases of about 20 cm and 180 cm, and a height of about 120 cm. The iron yoke has an octagonal shape, with two endcaps that can be opened vertically to access the detector.

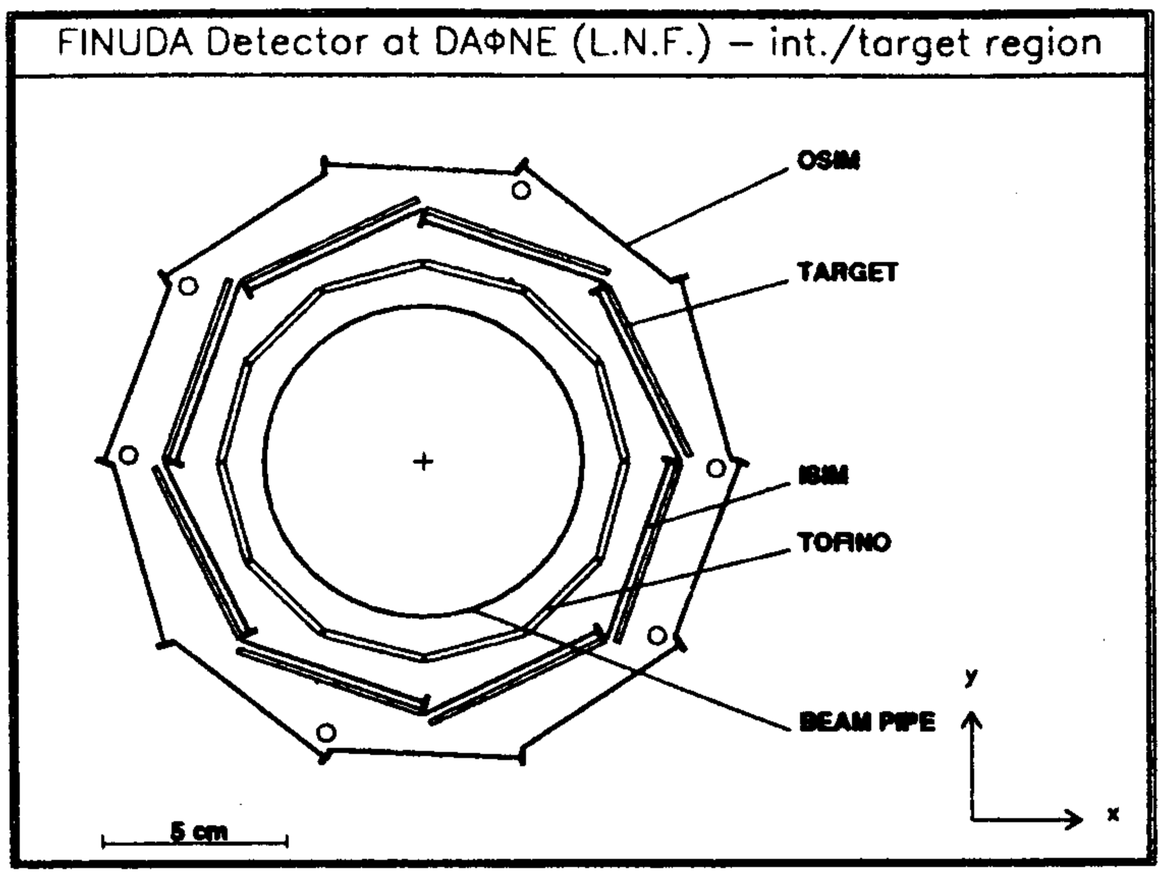


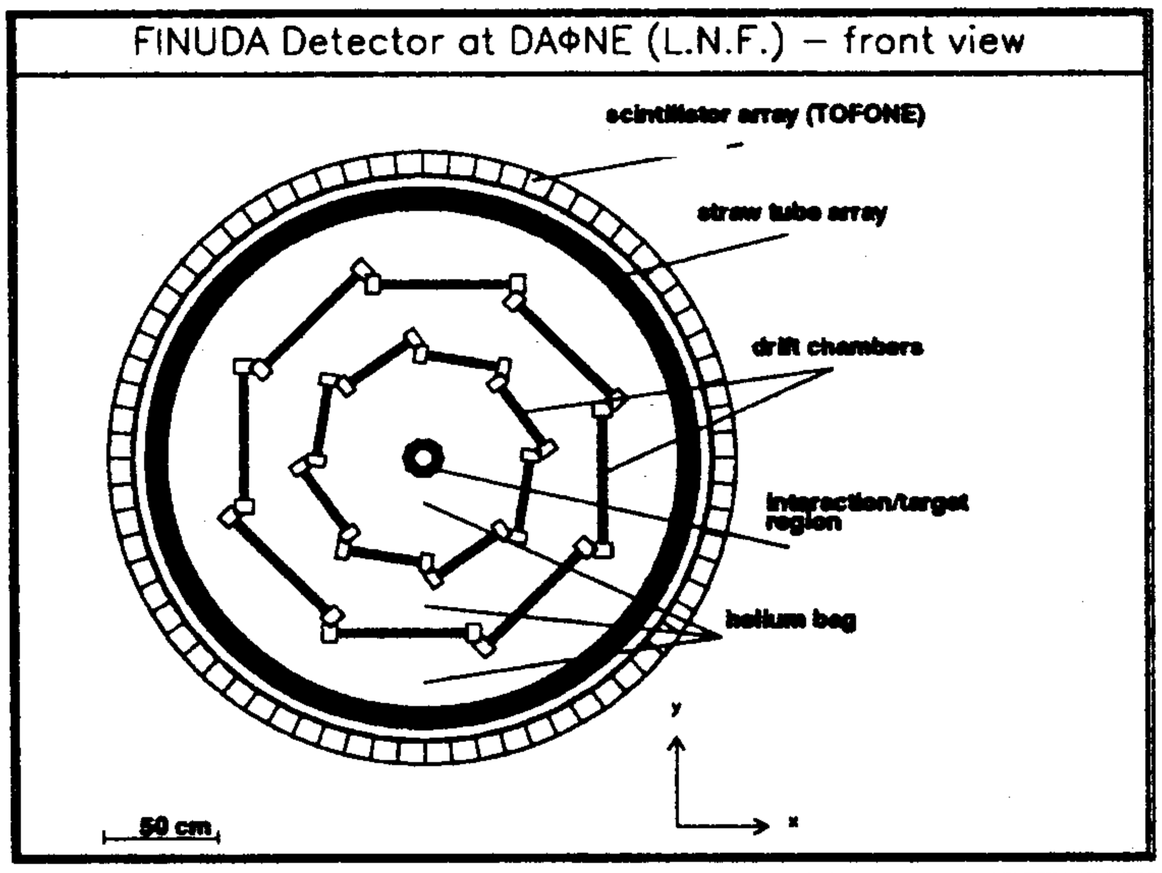


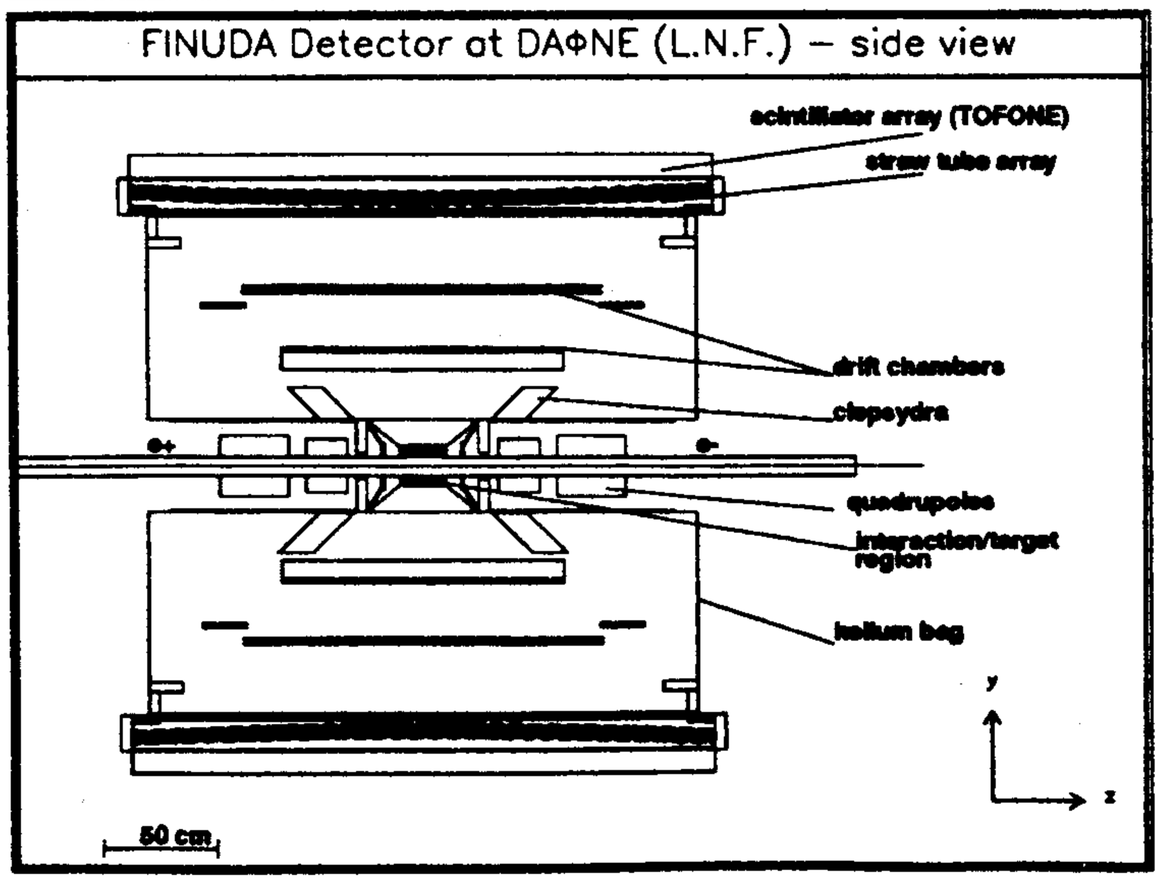


Figure 3: Interaction/target region (top); sketch of the FINUDA detector front view (center); and side view (bottom). *Clepsydra* is the support structure sustaining the detectors.

The cylindrical interaction/target region of FINUDA (fig.3) consists of the beam pipe, a scintillator barrel (TOFINO), an internal octagonal Si microstrip array (ISIM), and the nuclear stopping target. The above arrangement must:

1) identify $(K^+, K^-)$ pairs from $\phi$ decay for triggering by exploiting the back-to-back event topology and by identification through ionization energy loss $-(dE/dx)$ (TOFINO);
2) measure the $(K^+, K^-)$ coordinates before the nuclear target with $\sigma \sim 30-50\mu m$, provide particle identification by $-(dE/dx)$ , and have triggering capabilities (ISIM);
3) stop the monochromatic $K^-$ as near as possible to the external surface of the target;
4) measure the lifetime of hypernuclear states (TOFINO);
5) be radiation hard to cope with damage caused by Bhabha- and Touschek-scattered beam particles.

The thicknesses needed for the inner detectors are determined by the requirement of stopping the $K^-$ as close as possible to the outer surface of the target, taking also into account its energy straggling and $\sin^2\vartheta$ angular distribution. The target's octagonal shape allows one to use different materials simultaneously. The length of the interaction/target region is determined by the requirement of accepting all the $(K^+, K^-)$ pairs emitted from 45° to 135° along the $z$-coordinate from −3.5 cm to +3.5 cm, which corresponds to the fwhm of the $(e^+, e^-)$ interaction region. The resulting length of the target will be 17 cm and will allow an acceptance for $(K^+, K^-)$ of more than 90%.

The TOFINO consists of 12 strips, each 2.0 mm thick, 14 cm long and 2.5 cm wide, subtending a polar angle $\Delta\varphi = 30°$. The strips are arranged following a circumference of radius 5.5 cm and are read by hybrid photo multiplier tubes (HPMT). The HPMT's operate in the 1.1 T-magnetic field and are very compact.

The two silicon microstrip arrays ISIM (in the interaction/target region) and OSIM (in the outer tracker) are composed of 18 modules in total. Each module is made of three $300-\mu m$-thick, $52.6\,mm \times 65.4\,mm$ double-sided ($\rho$ and $\varphi$ strips) Si wafers bonded together. The pitch is $50\,\mu m$, and the strip width $6\,\mu m$ for a total of $4\times10^4$ strips. The external tracker, which consists of a ten-sided outer silicon microstrip detector (OSIM), two sets of planar low-mass drift chambers (LMDC) immersed in a He atmosphere, and an array of straw tubes (ST), has to:

1) measure the position of the prompt 270 MeV/c $\pi^-$ from the hypernucleus production very close to the target, thus determining the position of the $K^-$ stopping point and thereby correcting for the energy lost in the thin target, with a consequent improvement in momentum resolution (OSIM);
2) measure the second and third space points of the prompt $\pi^-$ trajectory in the $(\rho, \varphi)$ plane, with high resolution and maximal transparency (LMDC);

3) measure the fourth space point with good accuracy, and independently of the incident angle of the track due to the curvature caused by the magnetic field (ST).

The LMDC are two sets of planar drift chambers using a He-based gas mixture, each one with a $(1230 \times 396) mm^2$ (inner chambers) and $(1870 \times 686) mm^2$ (outer chambers) area. Measurement of the coordinate along the wire is made by means of charge division.

The ST array is composed of 2424 0.03-mm-thick aluminized mylar straws with an inner diameter of 15 mm, and a length of 255 cm. The straws are arranged in three superlayers, each one formed of two layers staggered by approximately half the diameter. The inner superlayer is axial, the two outer superlayers are stereo oriented at $\sim \pm 13^0$.

Finally, the outer scintillator array (TOFONE) will provide a fast logic signal for the DAQ trigger (multiplicity and coincidence of the prompt $\pi^-$ with the TOFINO signal) and neutron detection (with a ~15% efficiency). The TOFONE is composed of 72 slabs of plastic scintillator, 255 cm long and 10 cm thick, with read-out at both ends by 90° deflector prisms and lightguides funnelling the light signal to photomultipliers located in a low-field region outside the magnet.

## 3.2 Status of Subdetectors

### 3.2.1 Interaction/target Region

After tests with cosmic rays, the NE104 scintillator was selected for the internal scintillator barrel (TOFINO), since it provides light output in excess of 50 pe/mip. Two HPMT sample prototypes under test gave a 50 ps time resolution. Final assembly is scheduled by November 1995. Delivery of about 100 silicon wafers for the ISIM/OSIM detector is due by April 1995. Two full modules will be ready for testing at CERN and TRIUMF in September 1995.

### 3.2.2 Outer Tracker and TOF System

A $(115 \times 57)\, cm^2$ prototype low-mass drift chamber has been tested at CERN with a 5 GeV/c pion beam and a $He-iC_4H_{10}$ (70%-30%) gas mixture[22]. The space resolution was measured to be better than $100\, \mu m$ along the whole drift cell, with 98% average efficiency, while the coordinate along the wire was measured by charge division with a resolution of 0.61% of the wire length. Assembly of the detector is scheduled from May to December 1995.

An 8-channel straw tube prototype was tested at CERN with mip's in May 1994 using DME, and attained a $40 - \mu m$ space resolution [23]. A 160-channel prototype with axial and stereo superlayers tested at TRIUMF in December 1994 with a 300 MeV/c pion beam gave $\sim 100\, \mu m$ space resolution with the alternate gas mixtures studied ($Ar-C_2H_6$, $Ar-CO_2$)[24]. Assembly and quality control of about 2700 straw tubes will start at LNF in October 1995, with assembly inside the detector frame starting by March 1996.

Delivery is expected to be complete by November 1995 for all components (scintillators, light guides, and PMT) of the TOFONE array. A 80% efficiency light transmission to the

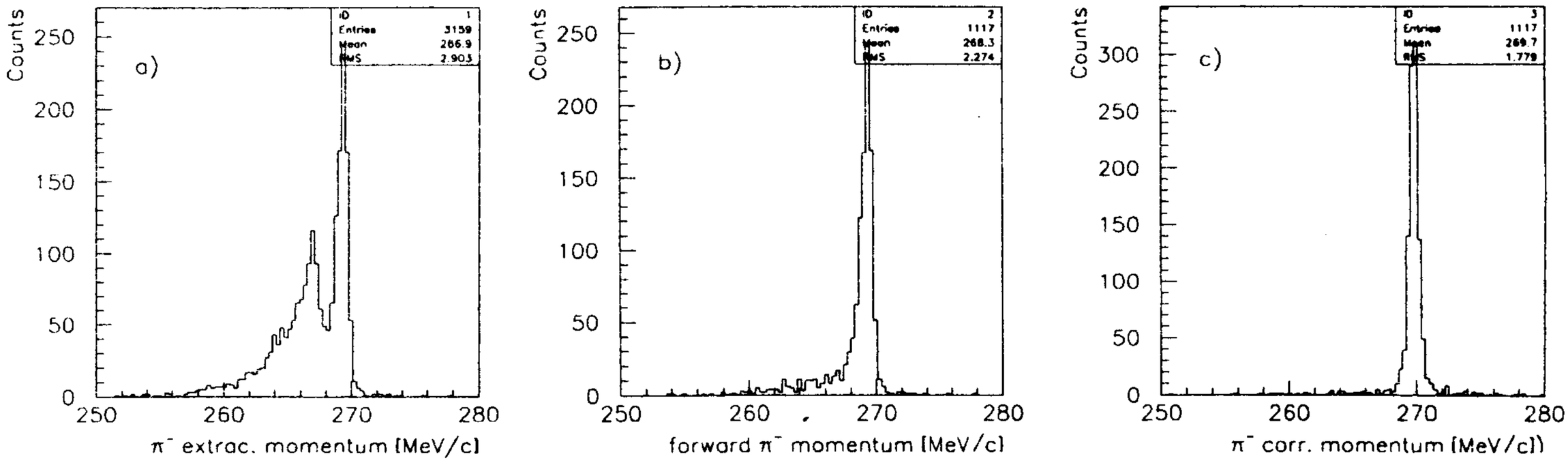


Figure 4: (a) Raw reconstructed momentum distribution of the prompt 270 MeV/c $\pi^-$; (b) only forward pions; (c) only forward pions, corrected for the energy loss in the target.

photomultiplier was found by using 90° conical deflector prisms. A 700 ps time resolution was obtained with a prototype bar.

### 3.2.3 The Superconducting Solenoid

The magnet contract was signed in December 1993 with Ansaldo, Genova, Italy. Coil and cryostat are expected to be completely assembled in December 1995. The magnet and end-caps will be transported assembled to LNF in June 1996, and installation in the experimental pit is scheduled to begin in mid 1996.

## 3.3 Performances

The characterization and testing of the FINUDA subdetectors described so far show how the design momentum resolution - the most crucial feature of the detector - is met with a safety margin. To demonstrate the resolving power in hypernuclear spectroscopy, a full simulation was carried out assuming the resolutions in table 3, all amply met, as shown by the test beam results.

Production of a hypernucleus state generating a 270 MeV/c prompt $\pi^-$ was fully simulated through the detector. The reconstructed raw momentum distribution (fig.4a) shows a shoulder at low energy, due to pions that cross the interaction/target region after being emitted, whose momentum is degraded by the material crossed. When selecting only the 'forward' pions (fig.4b), i.e., those not crossing back over the interaction/target region, the momentum resolution is of the order 0.3% fwhm. However, the momentum resolution for forward prompt pions can be further increased by exploiting the measurement of the $K^-$ stopping point by the ISIM and OSIM, and correcting their momentum by the thickness of target crossed. This is shown in fig.4c, where the mean of the distribution is now set to the 270 MeV/c generated momentum, and the width of the reconstructed spectrum is reduced to 0.25%.

Table 3: Space, time, and energy resolutions of the FINUDA subdetectors

| | Space rms | Time fwhm | Energy fwhm |
|---|---|---|---|
| TOFINO | - | $500\,ps$ | $-(dE/dx)$ 50 pe/mip |
| ISIM,OSIM | $50\,\mu m(x,y,z)$ | - | $-(dE/dx)$ 20% for K |
| LMDC | $100\,\mu m(x,y)$ | - | - |
| | 1% wire length $(z)$ | | |
| TOFONE | $5\,cm\,(z)$ | $500\,ps$ | - |
| ST | $100\,\mu m(x,y)$ | - | - |
| | $< 500\mu m(z)$ | | |

Table 4: Efficiency, rejection, and rates for production of hypernuclear states and background processes

| Efficiency for hypernucleus production events | |
|---|---|
| TOFINO BackToBack × dE/dx threshold | 80% |
| × TOFONE 10ns prompt coincidence | 46% |
| × TOFONE $\geq 1$ multiplicity (trigger eff. $\epsilon_T$) | 39% |
| × $\pi^-$ track has 4 hits | 29% |
| × forward $\pi^-$ (eff. $\epsilon_{\pi^-}$) | 13% |
| **Background rejection** | |
| Bhabha | $< 10^{-2}$% |
| $\phi \to K_S K_L$ | $(3 \pm 1) \times 10^{-2}$% |
| $\phi \to \rho\pi$ | $(4 \pm 1) \times 10^{-2}$% |
| $\phi \to \pi^+\pi^-\pi^0$ | $10^{-2}$% |
| $K^-$ interaction without hypernucleus | 7 % |
| **Trigger rates at $10^{32} cm^{-2} s^{-1}$** | **[Hz]** |
| Hypernucleus production ($10^{-3}/K^-_{stop}$ capture rate) | $8 \times 10^{-2}$ |
| Bhabha | $< 4 \times 10^{-2}$ |
| $\phi \to K_S K_L$ | $5 \times 10^{-2}$ |
| $\phi \to \rho\pi$ | $2 \times 10^{-2}$ |
| $\phi \to \pi^+\pi^-\pi^0$ | $10^{-3}$ |
| $K^-$ interaction without hypernucleus | 15 |

Table 5: Beam time required (in hours) at $\mathcal{L} = 10^{32} cm^{-2} s^{-1}$ to produce (with 10% and 20% statistical precision) hypernuclear states with capture rates from $10^{-3}/K^-_{stop}$ to $10^{-5}/K^-_{stop}$.

| Production rate | $10^{-3}$ 10% st. | $10^{-4}$ 10% st. | $10^{-5}$ 10% st. | $10^{-5}$ 20% st. |
|---|---|---|---|---|
| S/B=4/1 at $10^{-3}$ | 2.45 | 96 | 8000 | 2000 |
| S/B=8/1 at $10^{-3}$ | 1.8 | 56 | 4000 | 1000 |
| S/B=12/1 at $10^{-3}$ | 1.5 | 40 | 2300 | 575 |

### 3.4 Triggering Strategies, Rates, and Sensitivities

The FINUDA trigger selects $\phi$ decays into charged kaons, against decays into $K^o_S K^o_L$, Bhabha scattering, and cosmic rays. Bhabha events are naturally reduced by the geometrical acceptance covered by the TOFINO scintillator array $135^0 \leq \vartheta \leq 45^0$. The trigger requirements exploit the back-to-back topology of the $K^{\pm}$ pairs, their large $-(dE/dx)$ , and the coincidence with the prompt negative pion emitted from the hypernucleus formation as detected by the TOFONE:

- TOFINO back-to-back topology with dE/dx discrimination;
- TOFONE prompt $< 10ns$ coincidence and multiplicity $\geq 1$.

The prompt coincidence with TOFONE is dictated by the need to reject $\mu^+$ from $K^+$ decay. Table 4 shows typical triggering efficiencies for hypernuclear events and residual background contaminations. Hypernucleus formation rates at the initial luminosity $10^{32} cm^{-2} s^{-1}$ are shown in table 4, along with rates for background processes.

The rate of reconstructed hypernuclear events with resolution better than 1 MeV at $\mathcal{L} = 10^{32} cm^{-2} s^{-1}$ is given by the expression:

$$R({}_{\Lambda}Z) = R_{\phi} \times BR(\phi \to K^+K^-) \times \frac{N_{{}_{\Lambda}Z}}{K_{stop}} \times \epsilon_{\pi^-} \times \epsilon_{transp} \simeq 2.5 \times 10^{-2} s^{-1} \simeq 90\, events/hour$$

where $R_{\phi} = 5 \times 10^2 s^{-1}$, $BR = 0.49$, $N_{{}_{\Lambda}Z}/K_{stop} = 10^{-3}$ is the capture rate, $\epsilon_{\pi^-} = 13\%$ is the total efficiency for forward (high-resolution) prompt pions, and $\epsilon_{transp} = 80\%$ is the chamber transparency.

The FINUDA rate and resolution capabilities are summarized in table 5.

## 4 KLOE

The KLOE experiment [2] was proposed in April 1992; approved and funded at the beginning of 1993, construction of the detector began in 1994.

The principal aim of KLOE is the detection of direct CP violation in $K^0$ decays with a $10^{-4}$ sensitivity on $\Re(\epsilon'/\epsilon)$. For a comprehensive review see [25] and references therein, while a detailed status report can be found in [26]. More generally, KLOE should be regarded as a precision kaon-interferometer, since by studying the correlations between decays of $K^0_S K^0_L$ pairs, the interference in the decay intensities gives measurements of all eight parameters describing CP and CPT (if any) violations in the neutral kaon system, as described in length by Roberto Peccei at this Symposium [27].

[2] KLOE is on Internet `http://lnfmgr.lnf.infn.it/kloedef.html`

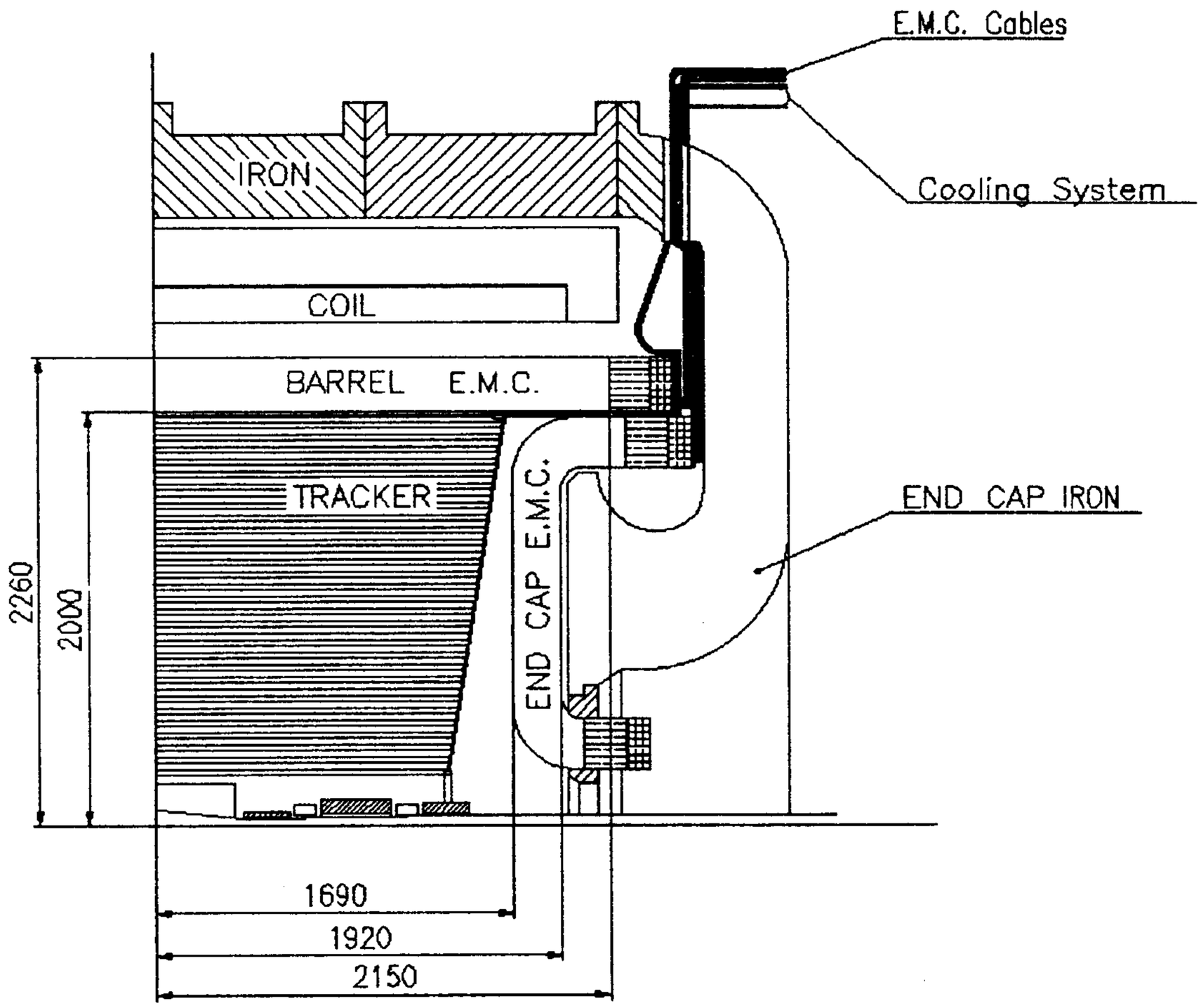


Figure 5: Cross-sectional schematics of the KLOE detector (one quadrant, side view). Dimensions are millimeters.

Other physics topics include rare $K_S^0$ decays ($10^{10}$ kaons per year will improve the sensitivity to branching ratios down to the $10^{-8}$ range), tests of Chiral Perturbation Theories, radiative $\phi$ decays, and $\gamma\gamma$ physics [28].

To reach the design sensitivity on $\Re(\epsilon'/\epsilon)$, a one-year statistics at full $DA\Phi NE$ luminosity is necessary. It is also necessary to control the detector efficiency for the decays of interest and to reject backgrounds from the copious $K_L^0$ decays to states other than two-pion.

The KLOE detector (fig.5) is a hermetic, $4\pi$ geometry apparatus: a cylindrical structure surrounding the beam pipe and consisting of a vertex chamber, a large drift chamber, an electromagnetic calorimeter with state-of-the-art energy and time resolution, and some particle identification, and a superconducting magnet.

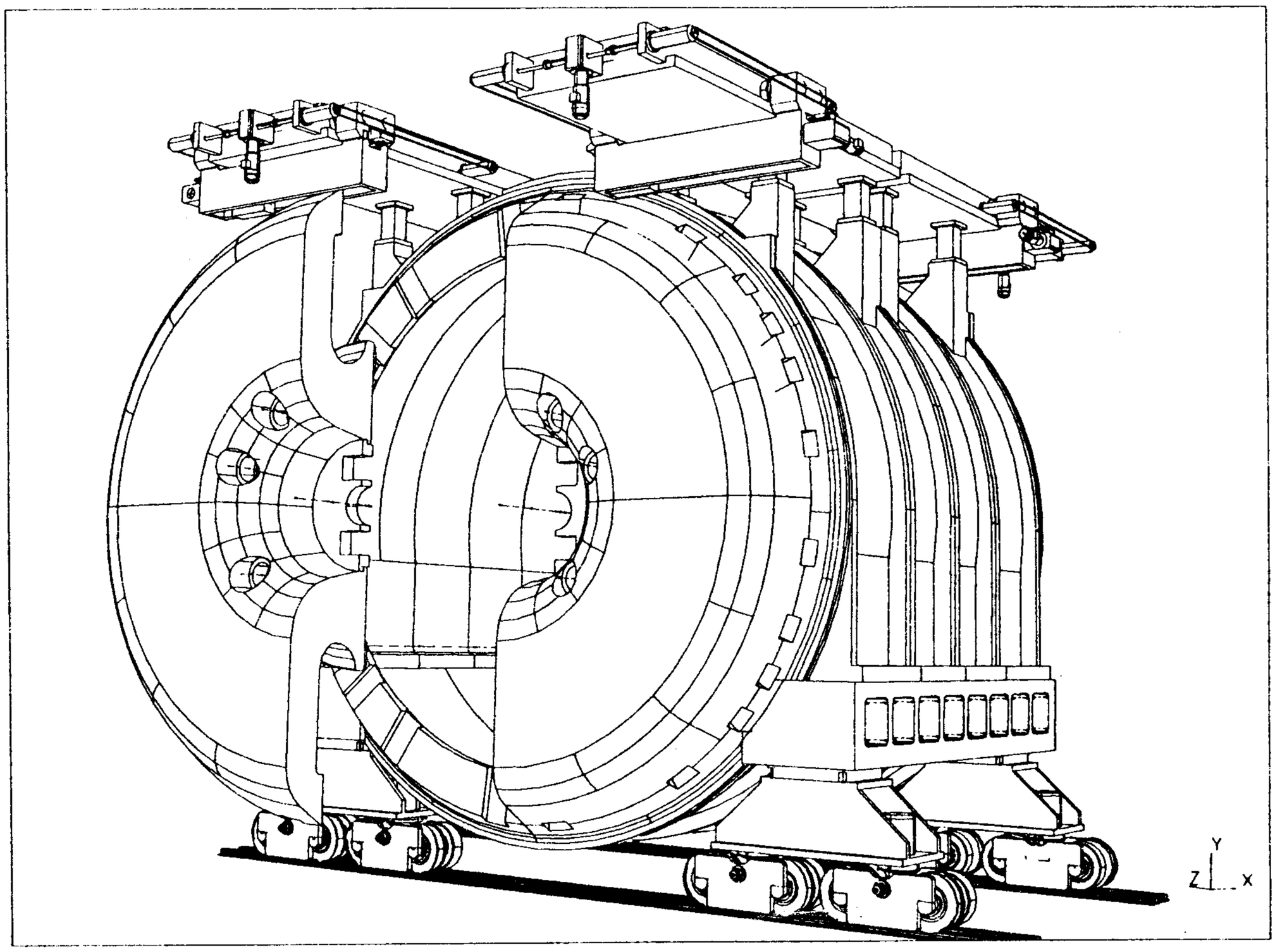


Figure 6: Overall view of the KLOE magnet.

## 4.1 Beam Pipe

A $500 - \mu m$-thick Be beam pipe with spherical shape at the KLOE interaction region is being developed by Brush-Wellman and K-TEK in parallel. The sphere radius (10 cm) is chosen to be much larger than the $K_S^0$ 6-mm decay length.

## 4.2 Magnet

Rejection of the contamination of the $K_L^0 \to \pi^+\pi^-$ sample is possible by measuring momenta with high resolution. Particularly vicious is the background of $K_{\mu 3}$ decays, kinematically overlapping the $\pi^+\pi^-$ decay at 250 MeV/c muon momentum. This overlap decreases as the cube of the magnetic field. On the other hand, tracking efficiency loss is observed when tracks spyralize in a high field. A optimal compromise is found at a 6-kG field generated by a superconducting solenoid [31].

## 4.3 Calorimetry

The KLOE calorimeter will reconstruct the $\pi^0\pi^0$ mode, determine the decay vertex space location, reject the $3\pi^0$ decay, and provide $\pi/\mu$ rejection. The technique employed is a Pb-scintillator sampling with 1-mm scintillating fibers embedded in very thin Pb grooved foils. Such a device has been extensively tested [29],[30] and demonstrated to provide good energy resolution, acceptable efficiency for photon energies down to 20 MeV, and spectacular time resolution: the time of arrival of one photon gives the flight path of the $K^0$ to an accuracy of 0.6 cm at a time resolution of 100 ps. Significant improvements have been achieved recently in the light output of the scintillating fibers [32] and on the photomultiplier [33] quantum efficiency. Eight out of twenty-four modules of the barrel are completed, and the machinery for constructing the endwalls is ready. A cosmic-ray stand is operational at LNF; the design of all the support mechanics is complete.

## 4.4 Tracking

A He-based, very transparent, drift chamber will reconstruct the $\pi^+\pi^-$ final state, reject the $K_{\ell 3}$ background, and determine the $K^0_S$ flight direction and the decay vertices; the choice of a drift chamber over a time-projection chamber was dictated by the need to sustain high event rates in the Bhabha region. The KLOE drift chamber has space resolution $\sigma_{\rho,\phi} = 200\,\mu m$ and $\sigma_z = 3\,mm$, 0.5% relative resolution on the transverse momentum, and a $\geq 98\%$ track reconstruction efficiency averaged over the $K^0_L \to \pi^+\pi^-$ decay. The mechanical structure is defined, and tender procedures are in progress to locate a manufacturer. The machinery to string some 27,000 wires is in construction. A further beam test on a 3.7-m-long prototype is planned for June 1995 at CERN.

## 4.5 Triggering and Background Rejection

To achieve the required statistical sensitivity, the entire $\phi$ event rate (5 kHz) has to be written on tape. The calorimeter will provide triggering for most of the decay channels of interest. The rejection of three neutral-pion decays relies on the calorimeter's hermeticity and efficiency for photons down to 20 MeV energy. The rejection of the $K_{\mu 3}$ decay over the $\pi^+\pi^-$ decay of interest is based on several kinematical variables and constraints. The high-resolution features of the tracking limits the residual contamination to $4.5 \times 10^{-4}$, at a 6 kG solenoidal field, with a 99.8% $\pi^+\pi^-$ efficiency.

# 5 Conclusions

A wealth of physics ranging from CP violation to hypernuclear studies is expected from $DA\Phi NE$ . The beginning of machine commissioning is planned for December 1996; construction of the detectors is well under way.

# 6 Acknowledgements

I gratefully acknowledge the help and information given by my colleagues on the $DA\Phi NE$ project team, KLOE collaboration and FINUDA collaboration, particularly G. Vignola, P. Campana, E. Botta, A. Feliciello, C. Guaraldo, S.Sarwar, and A. Zenoni. I especially benefitted from discussions with M. Preger, S. Bertolucci, F.L. Fabbri, and V. Lucherini. Thanks go to L. Benussi for his careful reading of the manuscript. Finally, I wish to thank the Organizing Committee for a perfectly enjoyable Symposium.

# References

[1] Proposal for a $\phi$-factory, the $\phi$-factory Study Group, Frascati Report 90/031(R), 1990.

[2] Review of Particle Properties, the Particle Data Group, Phys. Rev. **D50**, 1197, 1994.

[3] The $DA\Phi NE$ Physics Handbook, L. Maiani *et al.* (Eds.), published by SIS Laboratori Nazionali di Frascati, Frascati (1992).

[4] The Second $DA\Phi NE$ Physics Handbook, L. Maiani *et al.* (Eds.), published by SIS Laboratori Nazionali di Frascati, Frascati (1995).

[5] Proceedings II Work. on Phys. and Detector for $DA\Phi NE$ , R. Baldini *et al.* (Eds.), published by SIS Laboratori Nazionali di Frascati, Frascati (1995).

[6] G.Vignola, Proc. XXVI Int. Conf. on High Energy Physics, Dallas, 1992, J.R. Sanford (ed.), AIP Conf. Proc. No.272 (1993).

[7] for a recent and comprehensive review of $DA\Phi NE$ see: $DA\Phi NE$ Machine Project, the $DA\Phi NE$ project team, Proc. IV Europ. Part. Accel. Conf. (EPAC 94), London, 1994. Also Frascati Report LNF-94/055(P), 1994.

[8] Status Report on $DA\Phi NE$ , G.Vignola, ref.[5].

[9] Luminosity and Beam-beam Effects on the Electron-positron Storage Ring VEPP-2M, P.M. Ivanov *et al.*, Proc. of the III Adv. ICFA beam dynamics workshop, Novosibirsk 1989, I. Koop and G. Tumaikin (eds).

[10] Status of the Novosibirsk $\phi$-factory, L.M. Barkov et al., Proc. 1991 IEEE Part. Accel. Conf. S.Francisco (USA), May 6-9, 1991, p.183.

[11] Review of $\phi$-factories, M. Serio *et al., ibidem.*

[12] Design of the $e^+e^-$ Frascati Linear Accelerator for $DA\Phi NE$ , K. Whittam *et al.*, Proc. 1993 Part. Accel. Conf., Washington, D.C. (USA) 1993, 611-613.

[13] $DA\Phi NE$ Interaction Region Design, M. Bassetti *et al.*, *ibidem*, 2048.

[14] Background Evaluation in $DA\Phi NE$ , S.Guiducci, $DA\Phi NE$ technical note IR-6, 1995.

[15] Nuclear Physics at $DA\Phi NE$ , T.Bressani, Proc. Work. on Phys. and Detector for $DA\Phi NE$ , Frascati, April 9-12 1991, p.475 (G. Pancheri Ed.)

[16] Non-mesonic Decay of Hypernuclei and the $\Delta I = 1/2$ Rule, T. Bressani, ref.[4].

[17] Low-energy K-N Scattering with FINUDA, A. Olin, ref.[5].

[18] The Kaonic Hydrogen Puzzle, C. Guaraldo, ref.[5].

[19] FINUDA A Detector for Nuclear Physics at $DA\Phi NE$ , The FINUDA Collaboration (M. Agnello *et al.*), LNF preprint LNF-93/021(IR), 1993.

[20] FINUDA Technical Report, The FINUDA Collaboration (M. Agnello *et al.*), FINUDA Note 09/LNF/PUB/95, LNF preprint LNF-95/024(IR), 1995.

[21] FINUDA Status Report, A. Zenoni for the FINUDA Coll., ref.[5].

[22] Performance of a Large Area Drift Chamber Operating with a $He - iC_4H_{10}$ Mixture, M. Agnello *et al.*, to appear on Nucl. Instrum. and Methods A (1995).

[23] High Performance Tracking with Long Straw Tubes Using Dimethyl Ether, L.Benussi, *et al.*, Nucl. Instr. and Methods **A361**, 180-191, 1995.

[24] Test Beam Results and Gas System for the Straw Tube Detector, L.Benussi, *et al.* FINUDA note 18/BC/ST/95 (1995).

[25] KLOE at $DA\Phi NE$ , S.Bertolucci *et al.*, Nucl. Phys. B (Proc. Suppl.) **37A**, 43-50, 1994.

[26] Status of the KLOE Detector, J. Lee-Franzini, ref.[5].

[27] Overview of Kaon Decay Physics, R. Peccei, *these Proceedings.*

[28] Two-photon Interaction Measurements with the KLOE Small Angle Tagging System, F. Anulli *et al.*, LNF preprint 95-007(P), 1995.

[29] Lead/scintillating Fiber Electromagnetic Calorimeters with $4.8\%/\sqrt{E[GeV]}$ Energy Resolution in the 20-80 MeV Range, D. Babusci *et al.*, Nucl.Instr. and Meth. **A332** (1993) 444-458.

[30] Construction and Performance of the Lead-scintillating Fiber Calorimeter Prototypes for the KLOE Detector, A Antonelli *et al.*, Nucl. Instr. and Meth. **A354** (1995) 352-363.

[31] Oxford Instruments, Old Station Way, Eynsham-Witney OX81TL OXON, UK.

[32] POL.HI.TEC., Carsoli (AQ), Italy.

[33] Hamamatsu Photonics K.K., 438-01 Japan.